Estimation and Analysis of Sanding Length in Brush Sanding Specially Shaped Wood Products

Wang Baogang
Zhang Zhankuan
Peng Xiaorui

Abstract

Sanding is an important process in furniture production. Components with unconventional shapes are usually sanded by hand rather than by machine because heavy sanding makes machine sanding more difficult. However, manual sanding is inefficient and costly. Thus, a machine capable of sanding unconventionally shaped surfaces is needed.

In this study, we defined the cumulative sanding length *L* of a brush sander and built a numerical simulation model of *L* to analyze the problem of heavy sanding during surface brush sanding of specially shaped wood products. Based on our analysis of the motion and sanding process of a sander roller, we propose that the sanding strip should be bent when sanding flat surfaces and straight when sanding bulging surfaces. We also analyzed the effects of specific sanding parameters and the causes of heavy sanding. This research shows the following results: *L* increases with increasing theoretical contact length, the radius and rotational speed of the sander roller are proportional to *L,* feed rate is inversely proportional to *L,* and the *L* of a bulging point is 7.5 times greater than that of a flat surface. This difference is the main cause of heavy sanding, which is, in turn, mainly caused by different sanding strip patterns used when various parts of the component are sanded. This study provides a theoretical basis for using surface brush sanding for specially shaped wood products.

Sanding is a common process in the production of wood products, particularly during the varnishing process. Wood products often require sanding before varnishing and after each coat of primer. Sanding directly affects the quality of the final product (Xu 2011). Recently, a large number of specially shaped veneer components with convex or concave surfaces have appeared in wood products, such as wooden doors, windows, chairs, cabinet doors, crafts, and rattan products. The shapes of veneer components vary, and their surface curvatures are complex. These specially shaped components are difficult to sand by machine because cocked beads are susceptible to heavy sanding. Numerically controlled sanding machines do not meet production requirements because they are expensive and have high set-up costs and poor flexibility for specially shaped components. As a result, manual sanding is the most common method used for specially shaped components. However, manual sanding is inefficient, costly, and generates large amounts of dust, which impacts the health of workers (Zhang 2012). Against the backdrop of industrialization, manufacturers need a sanding machine that solves the problem of heavy sanding.

Brush sanding (Fig. 1) is a highly flexible grinding technology. A number of recently developed sanding machines are designed with brush sander rollers. However, the problem of heavy sanding remains unsolved. Up to the present, related research has focused on the relationship between technological parameters and surface roughness (Wang et al. 2010, Zhang and Zhang 2011), leaving the problem of heavy sanding unresolved. Therefore, determining the causes of heavy sanding and then solving this problem will be extremely useful. In heavy sanding, the shape of the components is changed or the film is worn out after sanding because of the high material removal rate that damages product quality. According to Archard's tribological equation (Rabinowicz 1965, Li et al. 2010), when a hard surface (supposing it has no abrasions) grinds a soft surface, the material removal rate on the soft surface is proportional to the force imposed on it and to the grinding distance that

The authors are, respectively, Postgraduate Student, Researcher, and Research Assistant, Dept. of Research Inst. of Wood Industry, Chinese Academy of Forestry, Haidian District, Beijing, China (wangbaogang113@126.com, zhangzk@caf.ac.cn [corresponding author], pengxr@caf.ac.cn). This paper was received for publication in July 2012. Article no. 12-00077.
©Forest Products Society 2012.
Forest Prod. J. 62(6):456–461.

http://prime-pdf-watermark.prime-prod.pubfactory.com/ | 2024-12-26

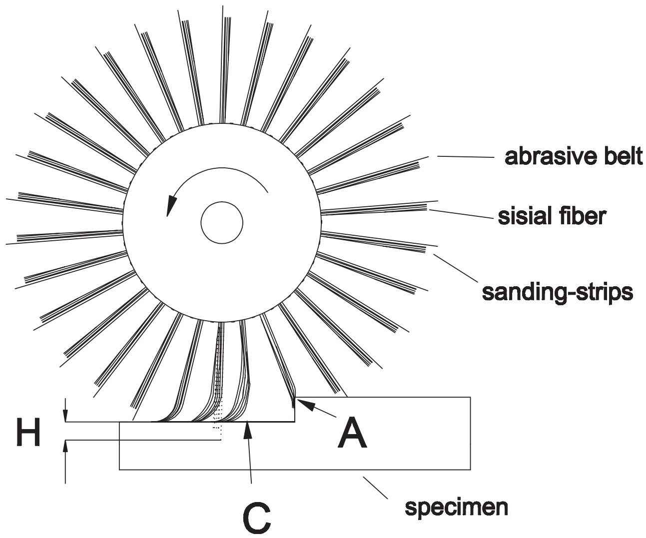

Figure 1.—Schematic diagram of brush sanding. A = the cocked beads; C = one point on the flat surface; H = theoretical contact length.

the hard surface moved on the soft surface and is inversely proportional to the hardness of the soft surface.

$$W = K_{\text{abr}} \frac{FL}{HV} \quad (1)$$

where

W = material removal rate,

F = force imposed on the soft surface,

L = grinding distance that the hard surface moved on the soft surface,

HV = hardness of the soft surface, and

K_{abr} = coefficient of wear.

Brush sanding involves grinding of an abrasive belt (hard surface) against wood or film (soft surface). The material removal rate is proportional to the grinding distance L. Brush sanding is a special type of sanding in which grinding distance is not calculated; thus analyzing the sanding process is difficult. This article analyzes the motion and sanding process to build a numerical simulation model of the cumulative sanding length L. Two points, A and C, were selected on the surface of a specially shaped work piece (Fig. 1). Point A represents protruding parts and the areas susceptible to heavy sanding. Point C represents the planar segment. In the sanding process, the grinding distances that the abrasive belt moved on point A and point C (or A/C moved on the abrasive belt; it is relative motion) are different; we calculate all grinding distances that the abrasive belt moved on point A and add them as L of point A. The same calculation is performed for L of point C. Based on the calculation, we analyzed the effects of sanding parameters and the causes of heavy sanding.

Structure and Motion

The brush sander roller, which has a special structure, is composed of evenly spaced sanding strips attached to a central wheel (Fig. 1). The sanding strips are composed of sisal fiber, which serves as a brace, and an abrasive belt used

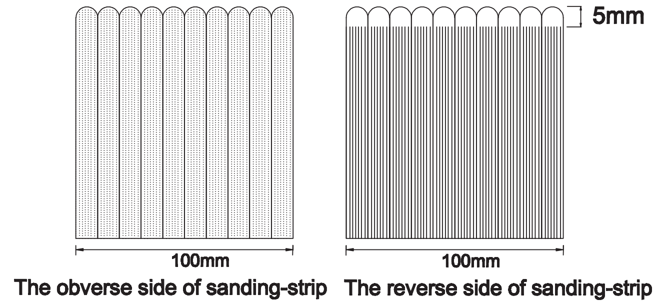

Figure 2.—Schematic diagram of sanding strips.

for sanding (Fig. 2). The abrasive belt, 5 mm longer than the sisal fiber, is cut into strips to improve its adaptability for specially shaped surfaces. In the sanding process, the bending angle of the sanding strips is determined by the shape of the specimen, to some extent adapting to the specially shaped surface.

Veneer components have various shapes and complex surface curvatures. For an expeditious study of the sanding process, the bulging point was simplified as a right angle (Fig. 1) between the cocked beads (A) and a point on a flat surface (C; Fig. 1).

Feed speed V and rotational speed ω are important brush sander roller parameters. The radius R of a brush sander roller, another important parameter, can be modified by adjusting sanding strips. Sanding strips are bent during the sanding process; the extent of such bending is determined by the distance from the top of the sanding strip to the surface of the specimen when the sanding strip is vertical, which is labeled as the theoretical contact length H (Fig. 1), yet another important parameter of brush sanding. The H of point A is different from the H of point C.

The top of the sanding strips is labeled as point B to analyze the motion of the sanding roller. The movement locus of point B is shown in Figure 3. The position of the sanding belt is at an angle OB at the beginning of the movement (where O is the center of the brush sander roller). The variable θ is used to represent angle OB deviated from the vertical position when the sanding roller rotates

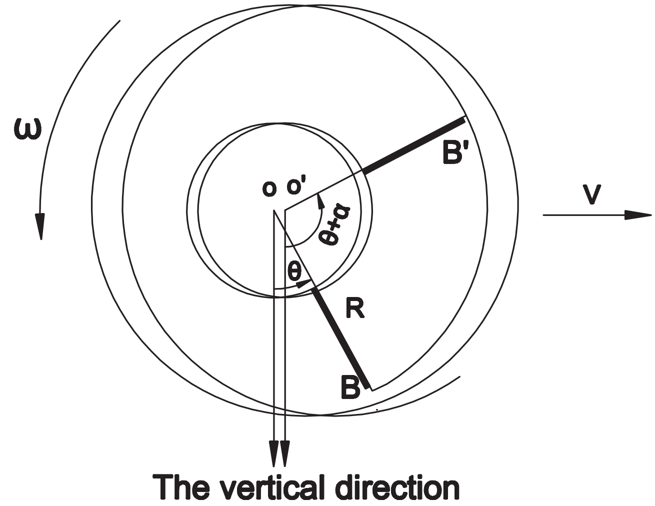

Figure 3.—Movement locus of point B. V = *feed speed;* ω = *rotational speed; B = top of sanding strips.*

http://prime-pdf-watermark.prime-prod.pubfactory.com/ | 2024-12-26

counterclockwise and moves in a specific direction. If the speed of the sanding roller is ω, and the feed speed is V, at time t, point O moves to point O′, point B moves to point B′, and the angle O′B′ that deviated from the vertical position becomes $\theta + \alpha$, which means that the rotated angle OB is α.

The horizontal direction of point C and the vertical direction of point A are set as the x axis and y axis, respectively. The distance between O and A in the x direction is set as x_0 in the initial position. To ensure that the sanding roller does not sand point A, x_0 must be set at a value greater than or equal to R.

The movement locus of O(x', y') is calculated using Equation 2.

$$\begin{cases} x' = -x_0 + V \times t \\ y' = R - H \end{cases} \quad (2)$$

where

x_0 = the distance between O and A in the x direction in the initial position,

V = feed speed,

t = the time of moving,

R = the radius of the sander roller, and

H = the theoretical contact length (the surface of C is the benchmark).

The rotation of angle OB is calculated using Equation 3:

$$\alpha = \omega \times t \quad (3)$$

where ω = rotational speed of the sanding roller.

The movement locus of B(x, y) is calculated using Equation 4:

$$\begin{cases} x = x' + R \times \sin(\alpha + \theta) \\ y = y' - R \times \cos(\alpha + \theta) \end{cases} \quad (4)$$

where θ = angle OB deviated from the vertical position.

Methodology

The following assumptions were made to calculate L:

- The differences between the sanding strips and the changes in the specimen were ignored.
- The effects of other sanding strips were ignored. If the sanding strips were too thick, they would squeeze and block each other. However, if the sanding strips were sparse, the effects on our data collection would be minimal. For the sake of convenience, the effects of other sanding strips were ignored.
- The effects of other parts involved in the sanding process were ignored. For example, if the sanding strip sanded point A, the sanding strip may be affected by the surface where point C is located, but the effect would be negligible and would therefore be ignored.

For point A, sanding number and length for every sanding strip were also computed to determine L. Points O, A, and B were occasionally aligned during sanding process. If these points did not align, the sanding strip would not be considered to have sanded point A. Figure 4 shows the relationships among O, A, and B when these points are aligned.

Although O, A, and B are aligned, (1) and (3) in Figure 4 are not considered to be in sanding status. In the case of (2), the length of AB is the length that sands point A under the

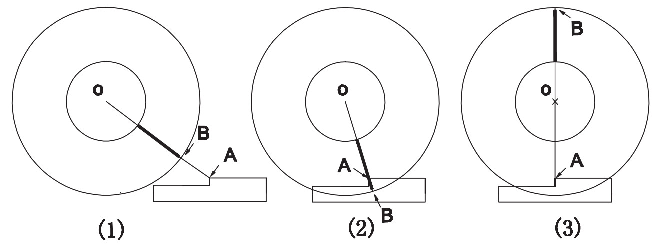

Figure 4.—Relationship among O, A, and B when these points are aligned. O = center of brush sander roller.

aforementioned assumptions. If (2) occurs, then sanding strip i is sanding point A the jth time. The parameter l_{ij} represents the length of AB. Equation 5 is used to calculate the L of point A.

$$L = \sum_{i=1}^{n_1} \sum_{j=1}^{n_2} l_{ij} \quad (5)$$

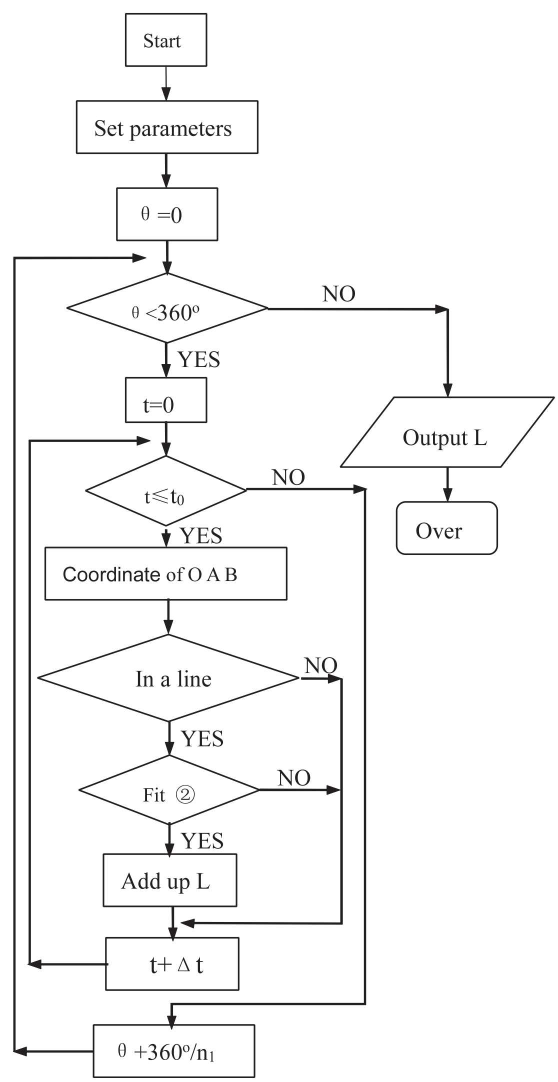

Figure 5.—Program flowchart for calculation of L.

http://prime-pdf-watermark.prime-prod.pubfactory.com/ | 2024-12-26

where

$n_1 =$ number of sanding strips and
$n_2 =$ number of sand for sanding strips.

For the brush sander roller in Figure 1, $n_1 = 30$. If the parameters of sanding were set, we could calculate the coordinates of O, A, and B, screen out the case of (2), and calculate the n_2, AB, and L of point A using a computer.

If the same method was used to calculate the L of point C, then the resulting bending shape of the sanding strips would be a folded line, which would contradict the facts. The sanding strips were bent while sanding point C and straight while sanding point A. The elastic modulus of the sisal fiber is greater than that of the abrasive belt, and the amount of sisal fiber is small; thus the abrasive belt is pressed against the sisal fiber. Only the 5-mm abrasive belt sanded point C, because it is 5 mm longer than the sisal fiber (Fig. 2).

Points O, C, and B were also occasionally aligned during sanding, and every time status (2) occurs, sanding strips sand point C. If CB $\leq$ 5 mm, sanding length would be the length of CB. If CB $>$ 5 mm, $l_{ij} = 5$ mm.

A sanding strip was assumed to be in a vertical position, that is $\theta = 0$, to simplify the computer program. The time span of the calculation $t_0 > (x_0 + R)/V$ was set to ensure the brush sander roller could not sand the specimen after the calculation. The interval of calculation Δt is set. Figure 5 shows the program flowchart.

Results and Discussion

In principle, the objective of brush sanding is to effectively sand most of the area of a specially shaped surface, whereas protruding parts are not heavily sanded. Point C is chosen to analyze sanding parameters. The parameters are set to $H = 10$ mm (the surface of point C being the benchmark), $R = 200$ mm, $\omega = 600$ rotations per minute (rpm), and $V = 6$ m/min, which are values frequently used in practice. The effects of these parameters on L of point C were analyzed, by changing three parameters to $x_0 = R$, $t_0 = 6$ s, and $\Delta t = 0.00001$ s and calculating L of point C using a computer. Figure 6 shows the effects of H, R, ω, and V on L of point C.

The following conclusions are drawn based on such calculations:

- L of point C is significantly affected by ω, where ω is the parameter constantly adjusted in actual production. When ω increases from 100 to 1,500 rpm, L of point C increases from 500 to 6,000 mm. Thus L of point C is directly proportional to ω and can be adjusted by ω within a wide range.
- L of point C is directly proportional to R, but the effect of R is insignificant. Figure 6 shows that when R increases by 40 mm, L of point C increases by only 200 mm. In actual production, the adjustment of R is a difficult operation requiring the replacement of sanding strips, and is thus rarely done. However, changing sanding strips results in a change in sanding forces, which could affect the quality of sanding and, therefore, requires further research.
- L of point C increases when H increases, but the trend stabilizes slowly. Under the given sanding parameters, if H is changed by 2 mm, L of point C changes by about 300 mm. H is constantly adjusted in actual production, which can change sanding force and must therefore be considered.
- V is inversely proportional to L of point C, and it can conveniently make large adjustments to L of point C without changing sanding force. However, the inversely proportional relationship is unfavorable for operation.

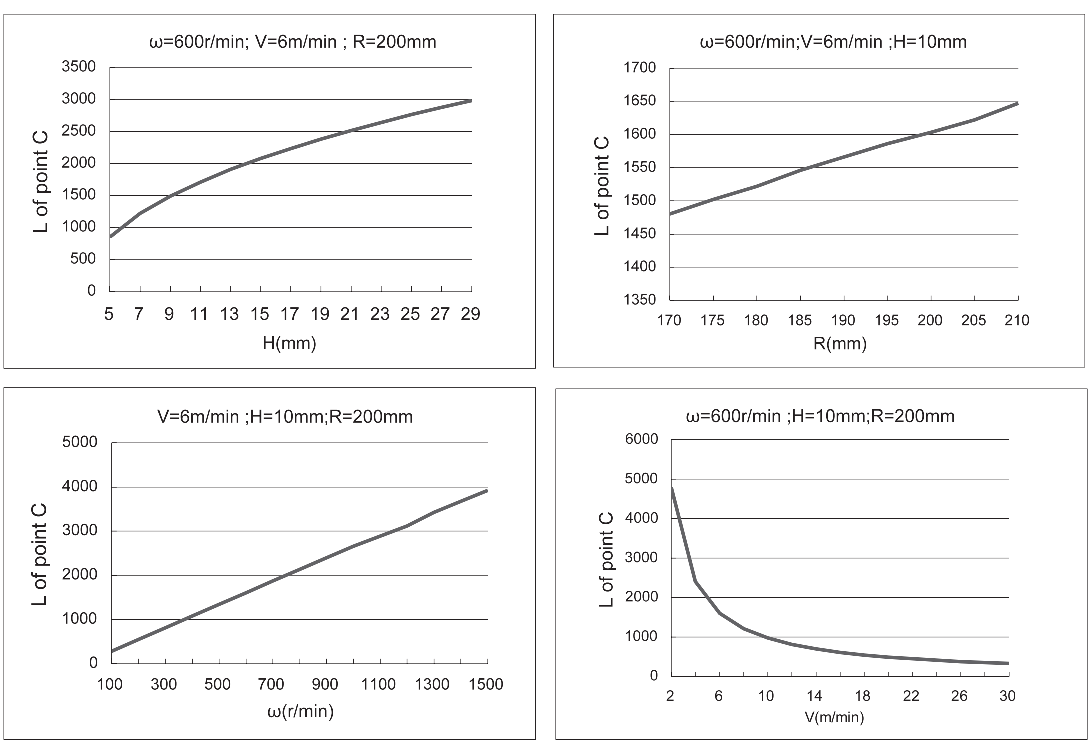

Figure 6.—Effects of specific parameters on L *of point C.* H = *theoretical contact length;* R = *radius of the sander roller;* ω = *rotational speed;* V = *feed speed.*

http://prime-pdf-watermark.prime-prod.pubfactory.com/ | 2024-12-26

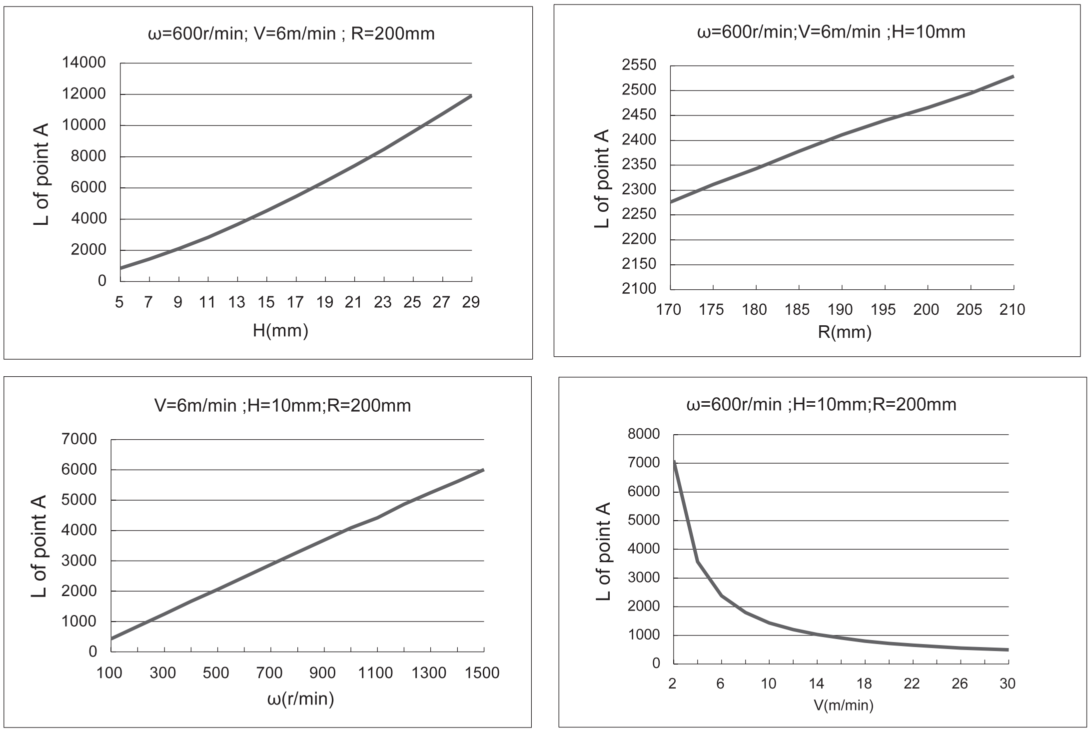

Figure 7.—Effects of the parameters on L *of point A.* H $=$ *theoretical contact length;* R $=$ *radius of the sander roller;* ω $=$ *rotational speed;* V $=$ *feed speed.*

Thus, operators need a better means of adjusting *L* of point C.

Based on the previous analysis, we confirm that brush sanding can meet the different needs of sanding force and *L* by adjusting *H, R,* ω, and *V*. Heavy sanding is the main problem in surface sanding of specially shaped wood products. Point A was chosen to analyze this problem. The computer-calculated results of *L* of point A are shown in Figure 7 with the following parameters: $H = 10$ mm (the surface of point A being the benchmark), $R = 200$ mm, $\omega = 600$ rpm, and $V = 6$ m/min (the same as in point C).

In following conclusions are drawn based on the calculation of and comparison between the *L* of point A and the *L* of point C:

- The effects of *R,* ω, and *V* on *L* are basically the same for points A and C. Thus, analysis of point C also applies to point A. However, under the given sanding parameters, *L* of point A is 1,000 to 2,000 mm greater than *L* of point C.
- The effects of *H* on *L* are different for points A and C. When *H* increases from 5 to 30 mm under the given sanding parameters, *L* of point A increases from 800 to 13,000 mm. *L* of point A increases with *H,* and the trend is exacerbated. However, when *H* increases from 5 to 30 mm, *L* of point C increases from 800 to 3,000 mm. *L* of point C increases with *H,* albeit more slowly (Fig. 6).
- For point C, if $H = 10$ mm, $R = 400$ mm, $\omega = 600$ rpm, and $V = 6$ m/min, *L* of point C is 1,600 mm. Supposing that point A has the same parameters as point C in actual production, except for being 19 mm higher than point C, $H = 29$ mm and *L* of point A is 12,000 mm, which is 7.5 times greater than *L* of point C. Therefore we conclude that this large gap between the *L* values of points A and C is the main cause of heavy sanding.
- The *L* of point A is greater than the *L* of point C for two reasons. First, point A is higher than point C, giving a larger *H* to point A. Second, the sanding strip is bent when sanding point C but straight when sanding point A. For point C, if $H = 29$ mm (the surface of C is the benchmark), $R = 200$ mm, $\omega = 600$ rpm, and $V = 6$ m/min, the *L* is 3,000 mm. Comparing this with the 12,000 mm (*L* of point A), we find that the difference in the sanding patterns of the sanding strips is the main reason for *L* of point A being much greater than *L* of point C.

Summary and Conclusions

This study investigated the brush sanding process of specially shaped surfaces, built a numerical simulation model of *L,* and analyzed the effects of several sanding parameters as well as the main cause of heavy sanding. We propose that the sanding strip must be bent when sanding flat surfaces, and straight when sanding bulging surfaces, The *L* of the sanding roller increases with increasing theoretical contact length. The radius and rotational speed of the sander roller are proportional to *L,* and the feed rate is inversely proportional to *L*. The different sanding patterns of sanding strips cause the *L* of specially shaped surfaces to be much larger than the *L* of flat surfaces. This difference is the main cause of heavy sanding. The results of this study provide a theoretical basis for use and

http://prime-pdf-watermark.prime-prod.pubfactory.com/ | 2024-12-26

improvement of surface brush sanding of specially shaped wood products.

Acknowledgment

This research was supported by the China Special Scientific Research Fund for Forestry Industry in the Public Interest (201204703).

Literature Cited

Li, X., Y. Chen, and L. Li. 2010. Abrasive belt sanding technology of wood-based panel. *Wood Process*. *Machinery* 3:44–48.

Rabinowicz, E. 1965. Friction and Wear of Materials. John Wiley, New York.

Wang, X., Z. Zhang, and J. Liu. 2010. A choice of sanding parameters for brush sanding machine. *Wood Process*. *Machinery* 5:4–7.

Xu, L. J. 2011. Fine sanding technology and equipments of veneer furniture components. *Furniture* 2:82–85.

Zhang, J. and Z. Zhang. 2011. Research about sanding parameters of the woodwork shaped surface based on taguchi method. *Wood Process*. *Machinery* 2:15–18.

Zhang, Z. 2012. Surface quality evaluation after sanding wooden door. *China Wood Ind*. 26(2):14–17.

http://prime-pdf-watermark.prime-prod.pubfactory.com/ | 2024-12-26